

Surface heating without moving any heat source

Mogulappa¹, Beesam Narasimha², MD. Yousuf³,

Assistant Professor¹, Associate Professor²,

Student³,

Department of Mechanical,

BRILLIANT GRAMMAR SCHOOL EDUCATIONAL SOCIETY'S GROUP OF INSTITUTIONS-

INTEGRATED CAMPUS

Abdullapurmet (V), Abdullapurmet (M), R.R Dt. Hyderabad-501505.

Abstract:

Experimental evidence supports the IREP's effectiveness. But, a new difficulty has emerged. The low quality of the produced spline shaft may be attributed to two primary factors. There is insufficient lubrication between the blank and rolling dies, and the unstable functioning of the air cylinder feed system makes in feed processes unpredictable. These are the essential issues that must be resolved by further studies of the IREP of spline shaft. Interference from Competing Interests Disclosure The authors have stated that they have no competing interests related to the research, writing, or distribution of this article. Funding The following institutions provided financial assistance for the development, writing, and/or distribution of this work; authors have indicated their participation in these activities. Both the Key Program (Grant No. 51335009) and the Basic Research Program of the National Natural Science Foundation of China helped fund these studies (Award No. 51305334).

1 Introduction

One of the most pressing problems in modern thermal engineering is the occurrence of phase change in commercial and industrial settings. In this context, exchanger systems of all types are under focus; they are expected to maximize efficiency while decreasing initial and ongoing expenses.

To that end, it's smart to focus on heat-tube based systems, which have a wide variety of applications including heat transfer, temperature maintenance, and heat flux management. They are used in solar collectors, heat exchangers, radiant wall panels, and other building components.

Heat tubes, also called heat pipes [1,2], are simple devices that transfer heat by convection and are filled with a working fluid and the vapors of this fluid. They are efficient heat conduits because they can carry a lot of heat for a long time and keep the temperature relatively stable. Unlike other systems, they can function efficiently without any additional

external energy.

Pumps and fans are used to propel the agent through the exchanger.

Figure 1 is a simplified diagram of the heat pipe, which is a thin tube lined with a structure designed with carefully selected geometrical/physical parameters, and which contains small amounts of a pressurized fluid, the boiling temperature of which is chosen taking into account the heat exchange conditions.

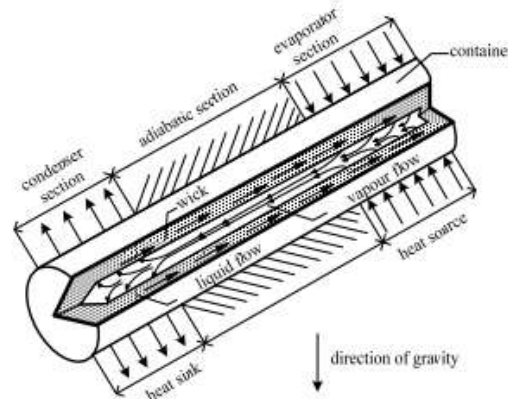


Figure 1. Diagram of a typical heat pipe with a schematic principle of operation

Different types of heat pipes exist, chiefly distinguished by the means by which condensation is transferred to the evaporator. Thermo siphons, heat pipes that can spin, and tubes with capillary structures that rely on capillary pressure to move condensate down their lengths are all distinct options.

Capillary-porous filling allows heat pipes to function in either a horizontal or vertical orientation. The value of capillary forces is far greater than the value of gravitational forces, and this is the underlying cause. Researchers have shown that using a variety of porous fillers may increase the effectiveness of these devices by increasing the capillary forces [4].

Using mesh structures, such as those made of metal fiber or powder and even those that are thermally sprayed, is one of the quickest and most popular ways to build the surface [5]. This category is

keenly interested in the capillary-porous and mesh architectures of metal fibers [6]. Thin fibers of different metals and their alloys are used to create metal-fiber covers. By strategically adjusting design factors including wall thickness, porosity, and skeleton conductivity, the heat transfer coefficient may be optimized for specific applications. It is possible to create capillary-porous structures with precisely the volume porosity and height that you need using commercially available mesh structures.

A capillary-porous liner is put within the heat pipe, with different functionalities at different points. On one end is an evaporator, which evaporates fluid by absorbing heat from its surroundings. On the other end, condensation happens in tandem with heat release into the environment. Exchangers with heat tubes can only operate so long before a crisis occurs [7]. When an evaporator becomes too hot, a phenomena called stagnation occurs, and restarting the process involves bringing the surface temperature down to where it would be under film boiling circumstances.

Transport and construction industry take advantage primarily of heat tubes with capillary structures [8]. They are used for:

- ground temperature stabilization around foundations and supports in arctic areas,
- defrosting of icy roads,
- the preparation of domestic hot water in heat exchangers,
- accumulation of solar energy in solar collectors,
- wall and under floor heating,
- heating ventilation air in combination with ecological energy sources.

Heat pipes have also been used to stabilize the temperature of the road surface [9]. For example, during the construction of the railway between China and Tibet they were placed in the permafrost sections. During thaw the ground under the railway sleepers thawed, which resulted in the collapsed tracks and broken rails. For these reason the pipes were designed to transfer the heat in one direction only, i.e. from the ground to the environment. The condensing section of the tubes was finned and projected above the surface of the ground, where it emits the heat extracted from the ground to the air. This caused the lowering of the ground temperature, which remains negative even during the thaw.

A similar solution was applied in the construction of the pipeline which transports oil from the north to the south of Alaska. A number of heat pipes that protect the ground from thawing and prevent pipe damage were installed along the route of the pipeline.

In the Nordic countries heat tubes are used for heating the road [10]. They are installed directly

beneath the road surface to maintain a constant, positive temperature of asphalt. Such solutions take advantage of geothermal energy available throughout the year [11], which can be accumulated to cover the peak demand [12].

Another application of large-size heat pipes is using them for heating the surface of bridges and overpasses, which in unfavorable climatic conditions become icy [13]. Such a system operates as a thermo siphon, where the supplied heat is associated with the convection movement. In this case there is no need for capillary porous layer between the section of the evaporator and the condenser, as the liquid phase condensed in the upper part flows down to the evaporator by gravity [14].

There are two types of solutions available here: passive and active systems. The passive system is the one in which the evaporator section is inserted in the ground at the depth where the temperature is constantly above 0°C. By contrast, the condenser section is placed directly under the surface, which should be protected from freezing. It is worth noting that this system further lowers the carrier temperature of the roadway in summer, increasing its durability. A simplified diagram of such a system is shown in figure 2. This system works spontaneously, without further supply of energy, which advantageously reduces the cost of operation [15, 16].

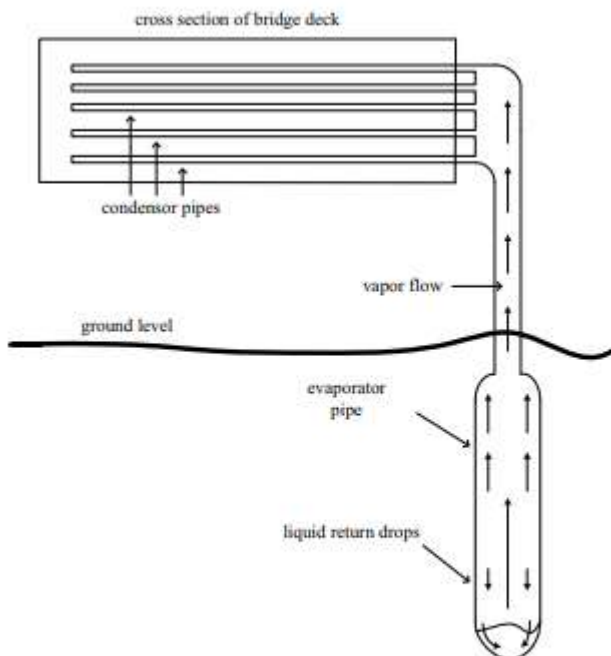


Figure 2. Diagram of the passive system of heating ground surface

In active systems operating with an external heat source e.g. a boiler, the systems equipped with heat pipes provide the stabilization of temperature, its

fine adjustment and the reduction of the maximum value (see figure 3).

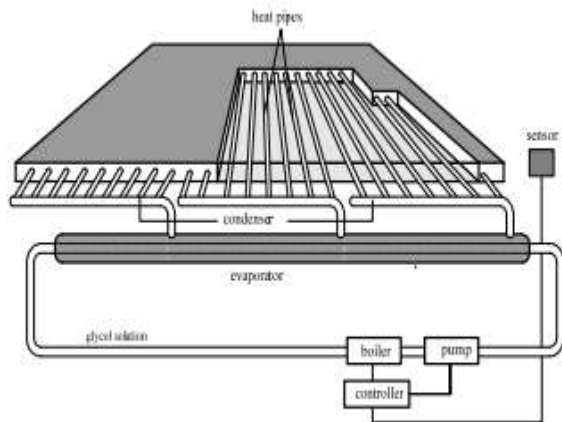


Figure 3. Active system diagram. Ground heating system that uses heat tubes and glycolic indirect system

The objective of this paper is to analyze the heat exchange at the boiling of ethanol as illustrated by no isothermal surface of a long copper fin coated with one layer of mesh and metal-fiber capillary-porous structure with the predetermined microstructure parameters.

2 Test facility

The tests were conducted on the stand, whose simplified diagram is presented in figure 4.

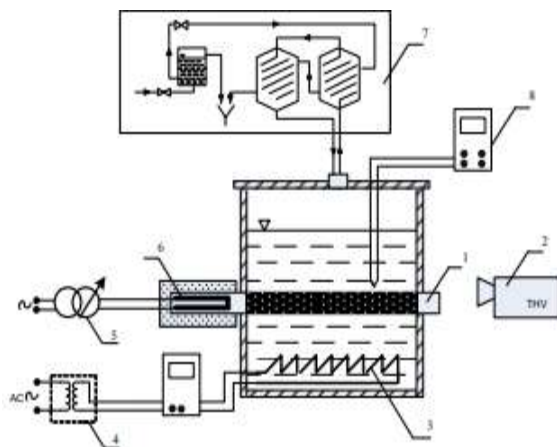


Figure 4. Diagram of the test facility for non-isothermal samples 1 – the examined element, 2 – the thermo vision camera, 3 – the auxiliary heater, 4 – the separation system with the control of supplied electric power, 5 – the main heater system with the electric power measurement, 6 – the main heater, 7 – the liquid supply and condensate recovery system, 8 – temperature measurement and control system

Its main part is a flat fin with a rectangular cross section. It is mounted between two side Bakelite plates, which provide a housing for the container filled with a boiling liquid. The fin is one-sidedly

covered with the structure intensifying the heat exchange (mesh layer with the metal-fiber capillary-porous structure) on the side of the liquid. The tests were performed in stationary conditions at the set temperature, different, however, for each series of measurements at the base of the fin. The necessary heat was supplied by the main electric heater powered from the autotransformer. In order to maintain boiling throughout the vessel, the auxiliary heater system was applied, with the heating part in the form of a resistance wire placed spirally at the bottom. Constant electric power supplied in the auxiliary heater system was maintained for all the measurement series. The vapour cooling and the condensate recovery were performed in a separate system of two radiators whose temperature was stabilized with district heating water in an open system.

The object of measurement is the surface temperature distribution across the fin from the outside, which was measured with an infrared camera VarioCAM®hr. The camera is equipped with an uncooled bolometric matrix with the 640 x 480 pixels image format. The device is designed to work in a long-wave range of infrared radiation of 7.5 \div 14 μm . The study was conducted with a standard camera lens (30 x 23°). The studied surface was evenly covered with black paint in order to ensure the optical uniformity of the outer surface of the tested samples.

The assembled measuring system permits assuming a single-dimensional phenomenon, i.e. the assumption that the change in temperature in relation to the fin thickness is negligibly small. This assumption is valid for the numbers of $\text{Bi} < 0.1$ [17]. The result of the study is a one-dimensional temperature distribution alongside the length of the fin along its axis.

Real objects emit not only their own, but also reflected radiation [18], which have a large impact on the final outcome measure [19]. Correct temperature reading requires an individual determination the emissivity of the investigated facility [20]. Therefore, before starting the measurement, calibration was performed examined surface radiation properties.

3 Research results and methodology

The tests were performed for a copper sample. A mesh structure with a metallic-fiber capillary-porous layer of the following parameters: height $h_w = 0.8 \text{ mm}$ and a volume porosity of $\sim 65\%$ was sintered on the sample. The structure was made from cut wire with the diameter of 0.05 mm and the fiber length of $\sim 3 \text{ mm}$, sintered in reducing hydrogen atmosphere [21]. Ethanol at atmospheric pressure was the heat-receiving agent. For comparative and calibration purposes a copper fin with a smooth surface was tested in identical

conditions [22].

The thermal field was obtained with the help of an infrared camera as a result of examining the outer surface of the analyzed part.

Figure 5 shows an example of a post-axial temperature distribution along the studied fin at the constant power of the main heater for two samples: the one with the smooth surface and the one coated with a mesh and capillary-porous structure. The Figure below shows that the application of the fibrous coating enhances the heat exchange as compared to a smooth surface. Due to a correspondingly large size, the cooling to the liquid boiling temperature occurs below the half-height point of the sample. This is observed for all the measurement series performed at a different electric power levels applied at the base of the main heater.

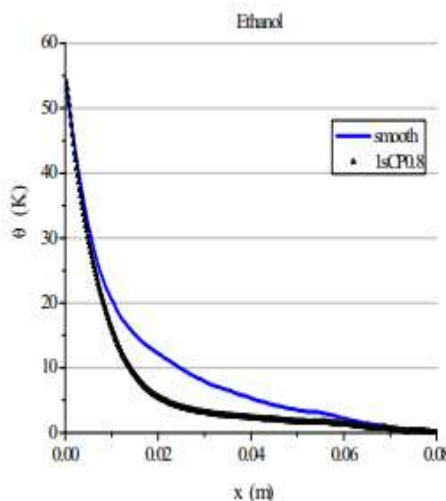


Figure 5. Temperature distribution on the copper fin along the center line at the constant power of the main heater for a smooth and capillary-porous sample with a layer height of 0.8 mm

The use of the infrared camera for measurement results in a large number of measurement points, permitting the application of the numerical differentiation combined with smoothing. Using this method, a derivative for the two examined samples, presented in figure 6, was determined with respect to the fin length. It is proportional to the amount of the transposed heat along the length of the element.

It should be noted that the value of the derivative is almost zero at a point below the half-height of the fin.

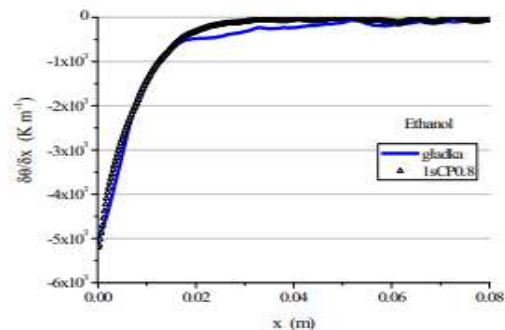


Figure 6. Temperature gradient versus length for the smooth sample and the sample coated with a single mesh layer with the capillary-porous structure

The derivative shown in figure 6 is used to calculate the locally transferred heat fluxes, and consequently to determine the boiling curve for the analyzed element with a non-isothermal surface. The result of the calculations for the smooth sample and the sample coated with mesh with the capillary-porous structure is presented in figure 7. The detailed calculation procedure is described in the paper [23].

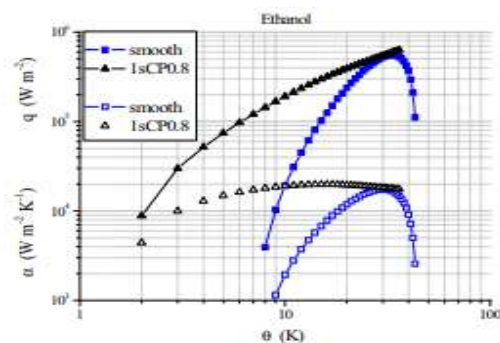


Figure 7. Boiling curve for the smooth sample and the sample coated with a mesh structure with a metallic-fibrous capillary porous layer

4 Conclusions

The relationship between the locally transmitted fluxes and the heat transfer coefficients for fins with a smooth surface and with a mesh and capillary-porous coating is the final outcome of the study carried out. For a smooth-surfaced sample, boiling in the nucleate pool begins at a superheating of 8 K, but for a sample with a structural covering, it begins at a much lower 2 K, as illustrated in figure 7. Maximum heat flow values have also been trending downward, suggesting a general trend toward safer operating temperatures. Table 1 contains local values of heat flux density at constant superheating. The difference between those values was calculated for both samples. While the difference initially grows, it decreases for higher values of superheating. The

maximum difference is noted in the case of 14 K superheat, for which $\Delta q = q_{\text{capillary-porous}} - q_{\text{smooth}} = 197.3 \text{ kW m}^{-2}$.

Tab. 1. Heat flux density at constant superheating

q (kW m^{-2})	$\theta = 10$ (K)	$\theta = 14$ (K)	$\theta = 19$ (K)	$\theta = 26$ (K)	$\theta = 29$ (K)
Q_{smooth}	19.3	80.3	206.9	425.0	502.8
$Q_{\text{capillary-porous}}$	190.0	277.6	374.3	487.1	530.7
Δq	170.7	197.3	167.4	62.1	27.9

References

1. D. Reay, A. Harvey, *Appl. Therm. Eng.*, 57 (2013)
2. L.L. Vasiliev, *Appl. Therm. Eng.*, 25 (2005)
3. H.N. Chaudhry, B.R. Hughes, S.A. Ghani, *Renew. Sust. Energ. Rev.*, 16 (2012)
4. T.M. Wójcik, *EPJ Web of Conferences*, 25 (2012)
5. M.G. Semena, A.N. Geršuni, V.K. Zaripov, *Viš. Škola*, Kiev, 1984
6. R. Pastuszko, *EPJ Web of Conferences*, 45 (2013)
7. T. Orzechowski, S. Wciliak, *Int. J. Heat Mass Tran.*, 73 (2014)
8. T.S. Winiewski, *Wymiana ciepła*, WNT, Warszawa, 1995
9. <http://en.sunpower.com.cn/>, [online 15.06.2015]
10. <http://www.alyeska-pipeline.com/>, [online 15.06.2015]
11. A. Manzella, *Geothermal energy*, *EPJ Web of Conferences*, 98 (2015)
12. T. Orzechowski, K. Stokowiec, *COW*, 44/1 (2013)
13. <http://www.smartbridge.okstate.edu/>, [online 15.06.2015]
14. P. Jakóbowski, *TChiK*, 4 – 5 (2009)
15. A. Nurpeis, *EPJ Web of Conferences*, 76 (2014)
16. P. Nemec, A. aja, M. Malcho, *EPJ Web of Conferences*, 45 (2013)
17. I.L. Pioro, W. Rohsenow, S.S. Doerffer, *Int. J. Heat Mass Tran.*, 47 (2004)
18. T. Kruczek, *Energy*, 91 (2015)
19. T. Kruczek, *Energy*, 62 (2013)
20. T. Orzechowski, *Exp. Therm. Fluid Sci.*, 31 (2007)
21. T. Orzechowski, A. Zwierzchowska, S. Zwierzchowska, *In. Ap. Chem.*, 6 (2009)
22. T. Orzechowski, A. Zwierzchowska, S. Zwierzchowska, *8-th European Conference of Young Research and Scientific Workers*, 2009
23. T. Orzechowski, *Exp. Therm. Fluid Sci.*, 8 (2007)